Report

Current Biology

Prolonged faunal turnover in earliest ants revealed by North American Cretaceous amber

Graphical abstract

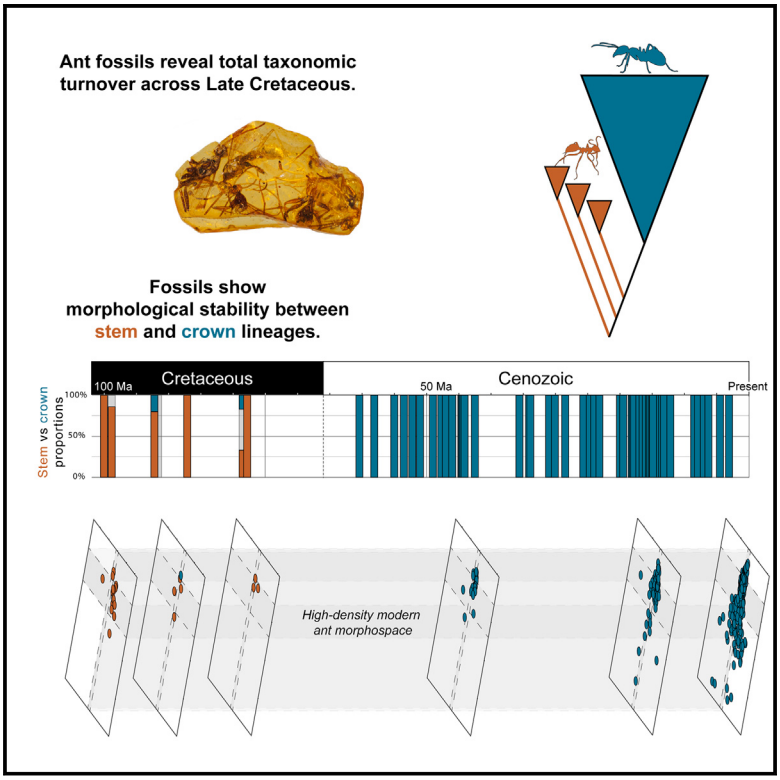

Authors

Christine Sosiak, Pierre Cockx, Pablo Aragonés Suarez, Ryan McKellar, Phillip Barden

Correspondence

christine.sosiak@oist.jp (C.S.), Ryan.McKellar@gov.sk.ca (R.M.), barden@njit.edu (P.B.)

In brief

Sosiak et al. describe the youngest stem ant fossils discovered from late Cretaceous North Carolina amber. Longevity and morphology of the Mesozoic ant assemblage demonstrates total taxic turnover through the late Cretaceous but general ant body plan stability over 100 million years, suggesting parallel but staggered adaptive radiations.

Highlights

- Youngest-yet (~77 Ma) stem ant fossils discovered from North Carolina
- Stem ant lineages demonstrate comparable generic longevity to crown ants
- General ant body plans have remained relatively constant across 100 Ma of evolution
- Taxonomic faunal turnover was prolonged across late Mesozoic

Sosiak et al., 2024, Current Biology *34*, 1–7
April 22, 2024
https://doi.org/10.1016/j.cub.2024.02.058

CellPress

Current Biology

CellPress

Report

Prolonged faunal turnover in earliest ants revealed by North American Cretaceous amber

Christine Sosiak,[1,2,6,7,*] Pierre Cockx,[3] Pablo Aragonés Suarez,[3] Ryan McKellar,[3,4,*] and Phillip Barden[2,5,*]
[1]Biodiversity and Biocomplexity Unit, Okinawa Institute of Science and Technology Graduate University, Okinawa 904-0495, Japan
[2]Department of Biological Sciences, New Jersey Institute of Technology, Newark, NJ 07102, USA
[3]Biology Department, University of Regina, Regina, SK S4S 0A2, Canada
[4]Royal Saskatchewan Museum, Regina, SK S4P 4W7, Canada
[5]Division of Invertebrate Zoology, American Museum of Natural History, New York, NY 10024, USA
[6]X (formerly Twitter): @paleANTologist
[7]Lead contact
*Correspondence: christine.sosiak@oist.jp (C.S.), Ryan.McKellar@gov.sk.ca (R.M.), barden@njit.edu (P.B.)
https://doi.org/10.1016/j.cub.2024.02.058

SUMMARY

All ~14,000 extant ant species descended from the same common ancestor, which lived ~140–120 million years ago (Ma).[1,2] While modern ants began to diversify in the Cretaceous, recent fossil evidence has demonstrated that older lineages concomitantly occupied the same ancient ecosystems.[3] These early-diverging ant lineages, or stem ants, left no modern descendants; however, they dominated the fossil record throughout the Cretaceous until their ultimate extinction sometime around the K-Pg boundary. Even as stem ant lineages appear to be diverse and abundant throughout the Cretaceous, the extent of their longevity in the fossil record and circumstances contributing to their extinction remain unknown.[3] Here we report the youngest stem ants, preserved in ~77 Ma Cretaceous amber from North Carolina, which illustrate unexpected morphological stability and lineage persistence in this enigmatic group, rivaling the longevity of contemporary ants. Through phylogenetic reconstruction and morphometric analyses, we find evidence that total taxic turnover in ants was not accompanied by a fundamental morphological shift, in contrast to other analogous stem extinctions such as theropod dinosaurs. While stem taxa showed broad morphological variation, high-density ant morphospace remained relatively constant through the last 100 million years, detailing a parallel, but temporally staggered, evolutionary history of modern and stem ants.

RESULTS AND DISCUSSION

Since their origin in the Paleozoic, insects appear to have experienced less extinction than their vertebrate or marine invertebrate counterparts.[4] While most clearly defined faunal turnover among insects occurs across the Paleozoic-Triassic boundary,[5] the ant fossil record chronicles a striking compositional transition that only recently has come into view. Unseen among 14,000 extant ant species are the products of an ancient doomed radiation that left no descendants. All modern ants derive from a common ancestor estimated to be ~140–120 million years in age[1,2]; however, stem ants—lineages that diverged prior to this common ancestor but are more closely related to modern ants than any other extant group of organisms[3]—are far more common in the early ant fossil record. The earliest known ants come from two approximately contemporaneous amber deposits dated to the Cenomanian (100–99 million years ago [Ma]) in France and Myanmar.[6,7] Stem ants are known across the Late Cretaceous from New Jersey amber (92 Ma), Taimyr amber in Siberia (~89–85 Ma), and Canadian Medicine Hat amber (~78 Ma).[8–10] Some stem ants, such as haidomyrmecine hell ants, which exhibit cranial horns and tusk-like mandibles, are extremely morphologically aberrant.[11] However, several taxa, such as the genera *Gerontoformica*, *Sphecomyrma*, and *Brownimecia*, are generalized; their stem lineage position is disclosed only by plesiomorphic features such as unreduced thoracic sculpturing in workers that is common among solitary aculeate wasps.[12] The stem ant fauna is a wide assemblage comprising both specialized and generalized taxa, all ultimately bound for extinction as their modern relatives continued to diversify into the Cenozoic.

The Cretaceous ant fossil record is interrupted by a 15-million-year fossil gap buffering the Cretaceous-Paleogene (K-Pg) extinction event that occurred at 66 Ma, during which all stem lineages went extinct; when the fossil record resumes in the Paleogene, crown lineages alone persist. This fossil gap obscures the timing and circumstances of stem to crown ant lineage turnover; moreover, almost all stem ant higher taxa are known from single localities, obscuring patterns of persistence over time. Here we report three taxa from Campanian deposits in North Carolina (USA), which represent the youngest glimpse yet into stem ant diversity. We combine these specimens with other morphological and phylogenetic fossil and extant data to demonstrate conclusive longevity in stem ants and ant body plan morphological persistence spanning 100 million years, providing insight into patterns of lineage replacement among lineages that shape terrestrial ecosystems today.[13]

Please cite this article in press as: Sosiak et al., Prolonged faunal turnover in earliest ants revealed by North American Cretaceous amber, Current Biology (2024), https://doi.org/10.1016/j.cub.2024.02.058

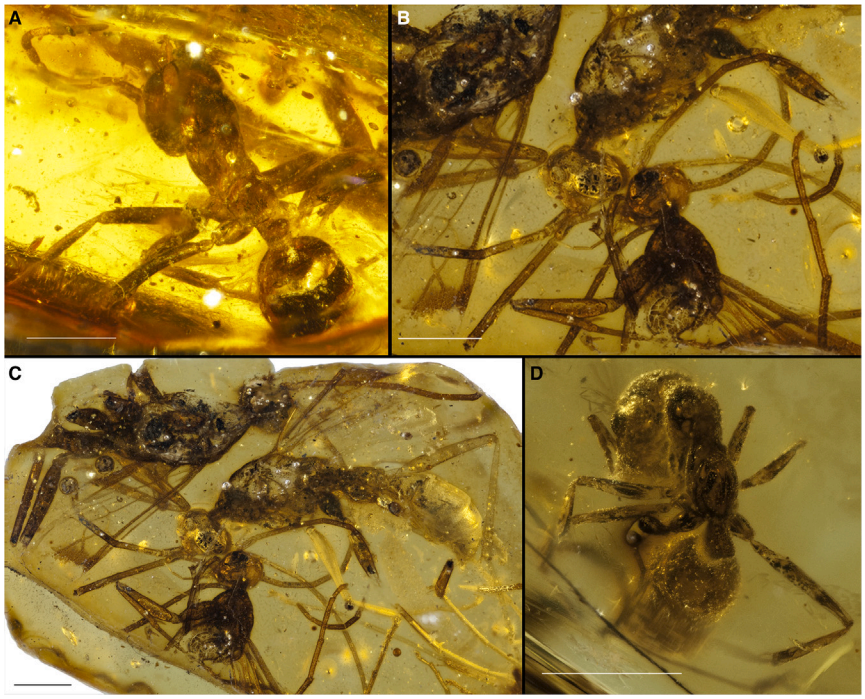

Figure 1. Campanian stem ants from North Carolina amber

(A) Dorsolateral view of worker *Sphecomyrma nexa* sp. nov. [holotype AMNH-NC-515].

(B) Dorsolateral close-up view of *Baikuris ocellantis* sp. nov. males head and mesosomal morphology [holotype AMNH-NC-MSE-2].

(C) Lateral view of *Baikuris ocellantis* sp. nov. males [holotype AMNH-NC-MSE-2].

(D) Dorsolateral view of worker *Brownimecia inconspicua* sp. nov. [holotype AMNH-NC-MSE-1]. Scale 1mm for all panels. See also Figures S1–S3.

Systematics

See STAR Methods for complete descriptions.

Family Formicidae Latreille, 1802[14]

Subfamily Sphecomyrminae Wilson and Brown, 1967[15]

Genus *Sphecomyrma* Wilson and Brown 1967[15]

Type species

Sphecomyrma freyi Wilson and Brown 1967[15]

Included species

Sphecomyrma freyi Wilson and Brown 1967[15]; *S. mesaki* Engel and Grimaldi 2005[16]; *S. nexa* sp. nov.

Sphecomyrma nexa sp. nov., Figures 1A, 2, and S1.

Diagnosis (brief)

Most similar to *S. freyi*; distinct from other species in intermediate size, the presence of an anteriorly pointed triangular spicule-like subpetiolar process, and a broader petiolar node.

Etymology

Derived from the root Latin word *nectere* meaning "to bind," in reference to *Sphecomyrma*'s status as the first described Mesozoic and stem ant species and its generalized morphology reflecting a "platonic ant" bauplan.

Genus *Baikuris* Dlussky, 1987[10]

Type species

Baikuris mandibularis Dlussky, 1987[10]

Baikuris ocellantis sp. nov., Figures 1B, 1C, and S2.

Diagnosis (brief)

Differentiated from other *Baikuris species* by large ocelli; toothless mandibles; forewing with partially formed 2r-rs that is largely obscured by fuscous area in wing membrane apical to pterostigma; 1m-cu is interstitial, with its anterior juncture located at the split between Rs and M.

Etymology

The specific epithet combines the Latin suffix *-antis*, or giant with ocellus, in reference to the large ocelli present within male members of the species.

Subfamily Brownimeciinae Bolton, 2003[17]

Genus *Brownimecia* Grimaldi et al., 1997[8]

Type species

Brownimecia clavata Grimaldi et al., 1997[8]

Brownimecia inconspicua sp. nov., Figures 1D and S3.

Diagnosis

Distinguishable from *B. clavata* by narrow and elongate mandibles with broad, blunt apices extending near base of opposing mandible; propodeum with posterior surface longer than dorsal surface; metasomal segment III slightly longer than segment II, with cinctus on segment III.

Etymology

The specific epithet comes from the Latin *inconspicuus*, or "hard to see," and refers to both the smaller compound eyes and mandibles without teeth found in this species.

Phylogenetic reconstruction, morphological persistence, and lineage longevity

Our phylogenetic hypotheses mirror previous assessments of Cretaceous and extant ants[3,11] (Figure 3B). Stem taxa are recovered outside of crown ants in unconstrained analysis. Proportional evidence from fossil deposits suggests stem lineage dominance throughout the Cretaceous (Figure 3A) while molecular estimates demonstrate that crown lineages accumulated only slowly throughout the Cretaceous; by the end of the Mesozoic, less than 100 extant lineages are estimated (Figure 3A).

We find that stem ants and crown ants do not occupy unique regions of the overall ant morphospace characterized through principal coordinate analysis (PCoA), though certain stem ant assemblages are more disparate than others (Figure 4A; Table S1). High-density extant PCoA morphospace largely encapsulates most stem ant taxa, with outliers at higher values of both principal coordinates 1 (PCo1) and 2 (PCo2) (Figures 4B and S4; Table S2). The Cenomanian assemblage, which is mostly dominated by hell ants, is more disparate than other Cretaceous assemblages and covers a wider breadth of PCo1 and PCo2 scores. This disparity is likely driven in part by increased sampling—Burmese amber is one of the most heavily sampled Cretaceous deposits worldwide—but additionally because of the abundance of hell ants within described species in this assemblage. The cranial morphology of hell ants is distinct

Please cite this article in press as: Sosiak et al., Prolonged faunal turnover in earliest ants revealed by North American Cretaceous amber, Current Biology (2024), https://doi.org/10.1016/j.cub.2024.02.058

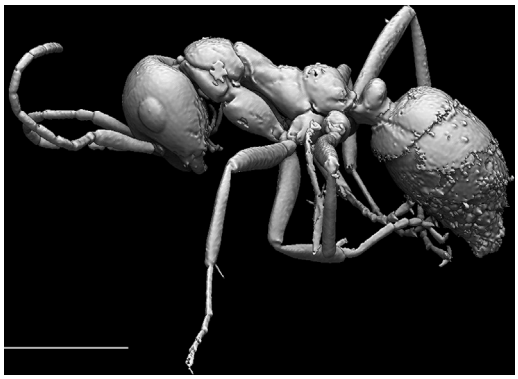

Figure 2. Lateral view of micro-CT reconstruction of *Sphecomyrma nexa* sp. nov. [holotype AMNH-NC-515]
Scale 1mm. See also Figure S1.

from other stem and crown lineages, although their post-cranial morphology is consistent with other stem taxa.[11] Stem ants recovered from Turonian and Campanian assemblages are more morphologically generalized, and their placement in high-density ant morphospace reflects this generalized bauplan. The sole exception is the Campanian hell ant *Haidoterminus cippus*, with morphology reflective of its Cenomanian relatives. The new North Carolina taxa, *S. nexa* and *B. inconspicua*, plot closely to the morphological mean of cumulative ant morphospace (Figures 4A, 4B, and S4; Table S2); similarly, they are proximate to their respective sister taxa *S. freyi* and *B. clavata* from New Jersey amber 92 Ma.

Ant body size (represented by PCo1 scores, with larger scores corresponding to larger body sizes) does not shift dramatically through time, though there is a shift to slightly larger body sizes in present-day ants; this increase is likely a reflection of sampling and taphonomic biases, rather than a biological shift (Figures 4A and S4; Tables S1 and S2). Ant cranial morphology (reflected by PCo2 scores, with larger scores indicating a squarer head shape versus smaller scores indicating a more anteroposteriorly extended shape) becomes increasingly boxier through time, most likely driven by the dominance of hell ants in the sampled Cenomanian assemblage, given their extreme cranial elongation associated with vertically aligned mandibles (Figures 4A and S4; Tables S1 and S2). Throughout the Cenozoic, crown assemblages do not undergo any marked morphological median shifts, though a greater overall degree of variation is present in more recent assemblages.

The three taxa reported here represent the only stem genera known from more than one fossil deposit (lineage longevity mean $\bar{x}$: 17.6 Ma; median $\tilde{x}$: 15 Ma), illustrating minimum longevity comparable to extinct ($\bar{x}$: 17.9; $\tilde{x}$: 16.9) crown genera throughout the fossil record (Figure 4C). Molecular ($\bar{x}$: 21.9; $\tilde{x}$: 21.5) and fossil estimates ($\bar{x}$: 29.3; $\tilde{x}$: 34) of extant crown genus age are similar, but the distribution of fossil estimates is more clumped, reflecting sampling bias from Dominican (~16 Ma) and Baltic (~34 Ma) amber in particular.

Stability of North American stem ant lineages

The morphological similarity between congeners from Turonian-age New Jersey amber and Campanian amber from North Carolina is striking, considering the 15 million years elapsed between the assemblages. With the inclusion of the North Carolinian species, the range of *Sphecomyrma* and *Brownimecia* is extended not only temporally but geographically, along the northeastern United States seaboard. Because of its mosaic-like body plan comprising putative plesiomorphic wasp- and ant-like features, speculation after the discovery of *Sphecomyrma*, the first known ant from the Mesozoic, suggested that it reflected the ancestral morphology of the earliest ants[15,20]; indeed, the similarity between *Sphecomyrma freyi* and morphology-based hypotheses of early ant ancestors persists as a classic example of ancestral phenotype estimation based on assumptions from morphology of extant lineages.[21] While it is possible that some aspects of *Sphecomyrma*'s morphology are reflective of the earliest ant ancestors, *Sphecomyrma* is among a paraphyletic assemblage of diverse stem ants (Figure 3B), which complicates this narrative. *Sphecomyrma* may have retained ancestral characters or converged upon a generalized ant phenotype; however, it is now clear that stem ants underwent a substantial adaptive radiation parallel with crown ant diversification[3] and that *Sphecomyrma* was a contemporary of nearly all extant ant subfamilies.

Baikuris is known from France (100 Ma), New Jersey (92 Ma), Siberia (~89–85 Ma), and North Carolina (77 Ma), making it the most widespread stem ant taxon and the only stem ant lineage aside from Haidomyrmicinae to span the Atlantic Ocean.[10] It additionally spans approximately 25 Ma, making it the most temporally persistent stem ant genus (Figure 4C), although the monophyly of *Baikurus* has not been assessed in a phylogenetic framework. The queens and workers of *Baikuris* are unknown, though it is possible some members of the genus are conspecific with already-described stem ant species, given the near-impossibility of associating fossil reproductive taxa and workers.[22] Considering the biogeographic overlap, they may be males of some hell ant genera, though the lack of *Baikuris* in haidomyrmicine-rich Kachin amber makes this less plausible. While our results provide the first insight into the deep time stability of stem ants, Early Eocene deposits bear genera that are extant today.[23,24] The extant genera *Gesomyrmex* and *Platythyrea* are both found in Oise amber (53 Ma),[25,26] *Camponotus* is found in Fushin amber (52 Ma),[27] and 26 extant genera are present in Baltic amber (44 Ma).[28–31]

The Cretaceous-to-Cenozoic ant faunal turnover

The ant faunal turnover across the K-Pg is markedly stable in terms of gross morphology; while there is phenotypic expansion overall post-K-Pg, the composition of Cenozoic and Mesozoic assemblages remains largely concentrated within extant high-density morphospace (Figure 4A). This type of faunal turnover—one where complete taxonomic restructuring is not paralleled by a gross phenotypic shift—is unusual relative to other faunal turnovers, including the theropod dinosaur-to-bird turnover[32] and replacement of mosasaurs by crocodylomorphs and sharks at the end of the Cretaceous[33] and shifts in molluscan assemblages from free-swimming to byssal forms during the Cenozoic.[34,35] That a stark transition in lineage composition over time is not accompanied by a clear morphological shift suggests that a generalized ant bauplan is capable of persisting across changing ecological niches and extinction events. While there are aberrant morphotypes, such as the haidomyrmicines,

Please cite this article in press as: Sosiak et al., Prolonged faunal turnover in earliest ants revealed by North American Cretaceous amber, Current Biology (2024), https://doi.org/10.1016/j.cub.2024.02.058

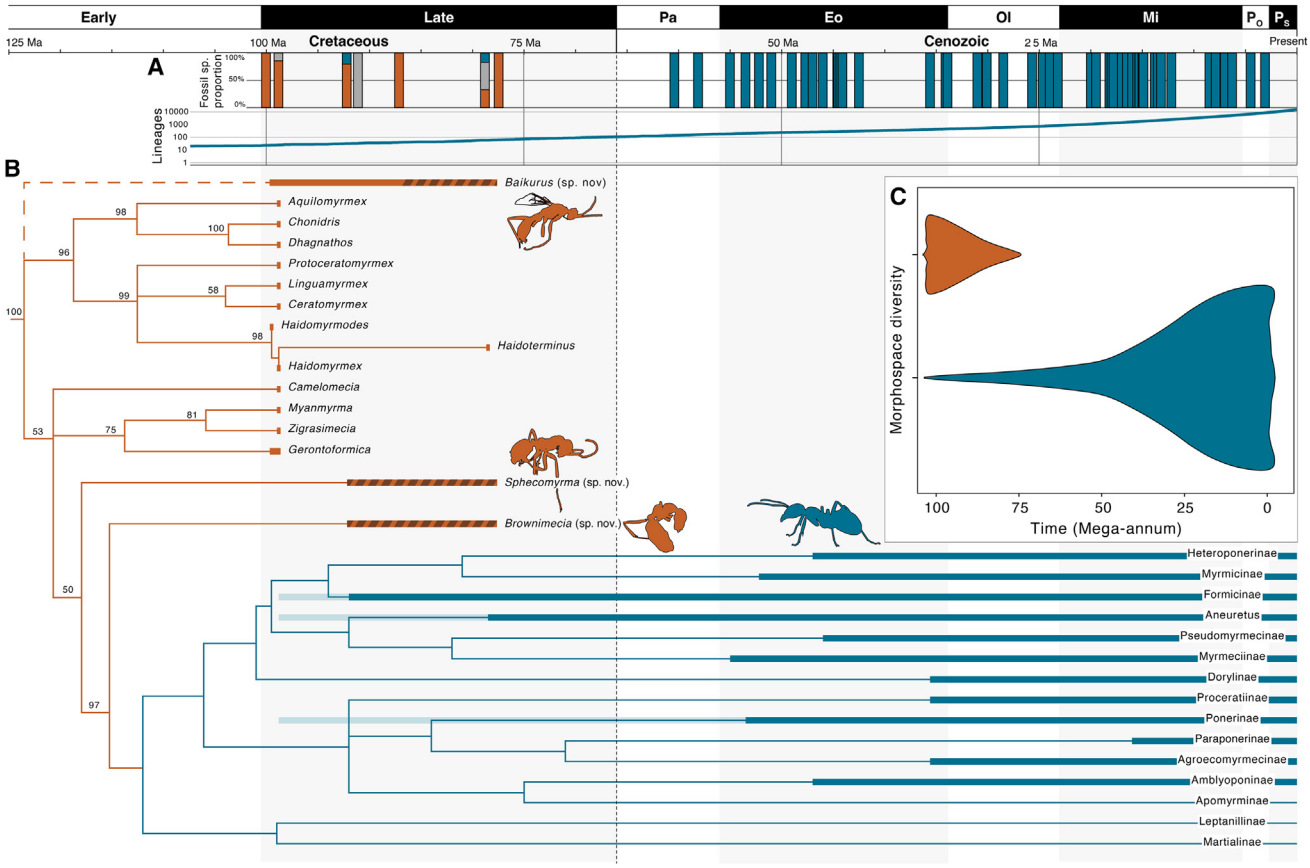

Figure 3. Phylogenetic reconstruction and comparative morphospace

(A) Top: percentage composition of crown (blue), stem (orange), and incertae sedis (gray) ants in all known ant-bearing fossil assemblages. Bottom: extant ant lineage accumulation over time derived from 14,512 terminal molecular phylogeny of Economo et al.[18]

(B) Phylogenetic reconstruction of stem (orange) and crown (blue) ant lineages. Broad bars on branches denote length of fossil history for genus or subfamily; hashed region denotes new range revealed by North Carolina amber; faint bars correspond with three putative crown-ants in 99 Ma Burmese amber that have not yet been described.[19] The genus *Baikuris* is only known from male specimens, and so its phylogenetic position has not been assessed; its placement is depicted with a dotted line.

(C) Comparative morphospace proportional occupation from principal coordinate analysis (PCoA) of all fossil and extant ant specimens through time; dimensions sourced from PCo1, which comprises 93.25% of total morphological variation (Figure 4A, see also Figure S4; Table S1, data from Data S1).

other morphologically modern stem ants coexisted with these forms.[16] It has been hypothesized that the development of eusociality was a major driver in crown lineage success relative to Cretaceous lineages.[36,37] Stem ants, however, were eusocial. Fossils of reproductive castes,[38] worker-pupae associations,[39] large worker aggregations,[3] and cross-species aggression[3] all confirm that these early lineages bore the hallmarks of eusociality. Crown lineages may have lived in larger colonies with more morphologically and behaviorally distinct reproductive castes, potentially providing a competitive advantage, but without more fossil evidence this hypothesis is speculative.

The lack of fossil deposits bracketing the Cretaceous-Paleogene extinction event make it difficult to accurately ascertain the proximate causes of this faunal turnover. Stem lineages may have been under competitive stress from crown lineages late in the Cretaceous, with lowered taxonomic diversity and abundance, and the K-Pg extinction event was an added ecological stressor that they were unable to survive. This pattern of decline and extinction would reflect a suppressive "press-pulse" effect, where environmental disturbances result in ecosystem alteration and declines in diversity and abundance of species, making them susceptible to sudden cataclysmic extinction events.[40] Indeed, this pattern has been observed in other faunal turnovers: metatherian mammals evolved in the Early Cretaceous but were likely competitively suppressed in the Late Cretaceous by the radiation of multituberculate eutherian mammals, with a comparatively higher rate of extinction in metatherian lineages across the K-Pg boundary than in eutherian lineages.[41] Similarly, the competitive suppression of belemnites by modern cephalopods may have made them more susceptible to final extinction across the K-Pg boundary,[42] and competition between ichthyosaurs and other large marine reptile taxa in the late Jurassic and Cretaceous may have resulted in ichthyosaur ecological marginalization and morphological constraint, predisposing them for extinction.[43]

A colocalized set of fossil deposits from the mid- and Late Cretaceous may provide further evidence of a pattern of competitive suppression and ultimate extinction. The Kachin

Please cite this article in press as: Sosiak et al., Prolonged faunal turnover in earliest ants revealed by North American Cretaceous amber, Current Biology (2024), https://doi.org/10.1016/j.cub.2024.02.058

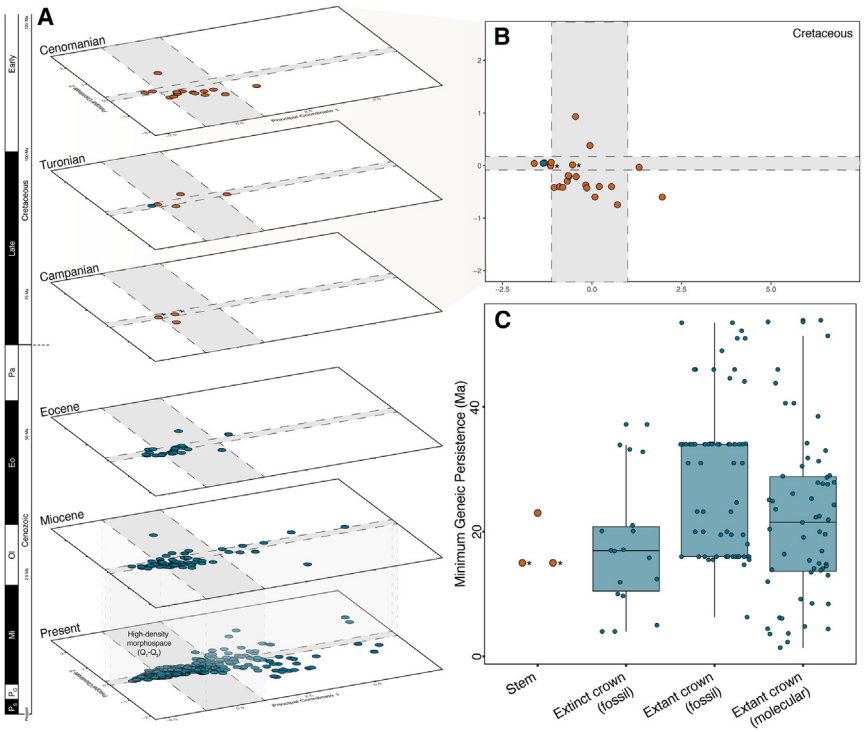

Figure 4. Chronomorphospace and generic longevity

(A) Chronomorphospace from principal coordinate analysis (PCoA) including stem (orange) and crown (blue) ant taxa. Light gray areas in each time slice represent the interquartile range between first and third quartiles for the present-day assemblage, denoting high-density ant morphospace. Asterisks denote *Brownimecia inconspicua* sp. nov. (left asterisk) and *Sphecomyrma nexa* sp. nov. (right asterisk) (PCo scores for *S. nexa* are PCo1 = −0.542, PCo2 = 0.012; scores for *B. inconspicua* are PCo1 = −1.153, PCo2 = −0.007). Sample sizes per timeslice: Cenomanian (n = 15); Turonian (n = 5); Campanian (n = 3); Eocene (n = 26); Miocene (n = 69); Present (n = 319) (see also Figure S4; Tables S1 and S2).

(B) Cretaceous chronomorphospace slice representing total Cretaceous morphospace inclusive from the Cenomanian through the Campanian (data from Data S1).

(C) Minimum genus-level lineage longevity in ants recovered from both fossil and molecular evidence (data from Data S2).

amber deposit (99 Ma) in present-day Myanmar is one of the most productive fossil ant deposits, bearing ~66% of known stem ant species and particularly high levels of haidomyrmicine diversity.[3,11,39,44] However, a newly described locality from Myanmar, so-called Tilin amber (71 Ma), reportedly bears solely crown lineage ants, albeit none described yet.[45] The compositional difference may be reflective of sampling biases, but it may also indicate that stem lineages were already declining in diversity and abundance or even extinct toward the end of the Cretaceous. Considering the high diversity of specialized haidomyrmicines in Kachin amber, it is also possible that morphologically aberrant lineages were most vulnerable; the North Carolina amber deposit as yet only bears stem ants and is only a few million years older than the Tilin deposit. This divergence suggests that turnover either did not occur at equal rates globally or that it occurred very rapidly across regions or habitats represented by amber deposit assemblages. Perhaps crown ants were diversifying more rapidly in Eurasia, outcompeting local stem ant species, or perhaps North American lineages such as *Sphecomyrma* and *Brownimecia* were more generalist in their life habits than specialized haidomyrmicines, reducing extinction risk.[46]

Faunal turnovers from the Mesozoic to the Cenozoic are not restricted to ants but have been observed in other insect and arthropod lineages. Spider lineages are distinct across the K-Pg boundary, with the Mesozoic faunas dominated by multiple stem families that are extinct by the end of the Cretaceous.[47] It is also argued that most insect extinction events throughout deep time are instead faunal turnovers, with high rates of both extinction and speciation marking biotic replacement in lineages.[5] Considering their small body sizes, ecological breadth, and short generation times, further investigation into extinction patterns in arthropod lineages may reveal that faunal turnover, rather than mass extinction, is the rule.

STAR★METHODS

Detailed methods are provided in the online version of this paper and include the following:

- KEY RESOURCES TABLE
- RESOURCE AVAILABILITY
  - Lead contact
  - Materials availability
  - Data and code availability
- EXPERIMENTAL MODEL AND SUBJECT DETAILS
- METHOD DETAILS
  - Specimen preparation
  - Specimen descriptions
- QUANTIFICATION AND STATISTICAL ANALYSES
  - Phylogenetic reconstruction
  - Lineage longevity estimates
  - Morphometric analyses

SUPPLEMENTAL INFORMATION

Supplemental information can be found online at https://doi.org/10.1016/j.cub.2024.02.058.

ACKNOWLEDGMENTS

We thank Morgan Hill for facilitating access to the American Museum of Natural History micro-CT scanning resources within the Microscopy and Imaging Facility. We also thank Victor Krynicki for donating specimens F002518 and F002519 to the Snow Entomology Museum Collection at the University of

Kansas, and we thank Michael Engel for facilitating access to the collection and assisting with specimen identifications. Support was provided by the Natural Sciences and Engineering Research Council of Canada (NSERC grant 2015-00681). Pierre Cockx was supported by an NSERC Discovery Grant held by Ryan McKellar and by the Friends of the Royal Saskatchewan Museum (Graduate Scholarship). Pablo Aragones Súarez was supported by a Mitacs Globalink Research Internship.

AUTHOR CONTRIBUTIONS

Conceptualization: C.S., P.C., P.A.S., R.M., and P.B.; data curation: C.S., P.C., P.A.S., R.M., and P.B.; statistical analysis: C.S. and P.B.; investigation: C.S., P.C., P.A.S., R.M., and P.B.; visualization: C.S., R.M., and P.B.; writing - original draft: C.S., R.M., and P.B.; writing - review & editing: C.S., P.C., P.A.S., R.M., and P.B.

DECLARATION OF INTERESTS

The authors declare no competing interests.

Received: September 21, 2023
Revised: December 13, 2023
Accepted: February 23, 2024
Published: March 22, 2024

REFERENCES

1. Borowiec, M.L., Rabeling, C., Brady, S.G., Fisher, B.L., Schultz, T.R., and Ward, P.S. (2019). Compositional heterogeneity and outgroup choice influence the internal phylogeny of the ants. Mol. Phylogenet. Evol. *134*, 111–121.
2. Moreau, C.S., and Bell, C.D. (2013). Testing the museum versus cradle tropical biological diversity hypothesis: phylogeny, diversification, and ancestral biogeographic range evolution of the ants. Evolution *67*, 2240–2257.
3. Barden, P., and Grimaldi, D.A. (2016). Adaptive radiation in socially advanced stem-group ants from the Cretaceous. Curr. Biol. *26*, 515–521.
4. Labandeira, C.C., and Sepkoski, J.J., Jr. (1993). Insect diversity in the fossil record. Science *261*, 310–315.
5. Schachat, S.R., and Labandeira, C.C. (2021). Are insects heading toward their first mass extinction? Distinguishing turnover from crises in their fossil record. Ann. Entomol. Soc. Am. *114*, 99–118.
6. Nel, A., Perrault, G., and Néraudeau, D. (2004). The oldest ant in the lower Cretaceous amber of Charente-maritime (SW France) (Insecta: Hymenoptera: Formicidae). Geol. Acta: an International Earth Science Journal *2*, 23–30.
7. Dlussky, G.M. (1996). Ants (Hymenoptera: Formicidae) from Burmese amber. Paleontologicheskii Zhurnal *30*, 449–454.
8. Grimaldi, D.A., Agosti, D., and Carpenter, J.M. (1997). New and rediscovered primitive ants (Hymenoptera, Formicidae) in Cretaceous amber from New Jersey, and their phylogenetic relationships. Am. Mus. Novit. *3208*, 43.
9. McKellar, R.C., Glasier, J.R., and Engel, M.S. (2013). A new trap-jawed ant (Hymenoptera: Formicidae: Haidomyrmecini) from Canadian Late Cretaceous amber. Can. Entomol. *145*, 454–465.
10. Dlussky, G.M. (1987). New Formicoidea (Hymenoptera) of the Upper Cretaceous. Paleontologicheskii Zhurnal *20*, 146–150.
11. Barden, P., Perrichot, V., and Wang, B. (2020). Specialized predation drives aberrant morphological integration and diversity in the earliest ants. Curr. Biol. *30*, 3818–3824.e4.
12. Boudinot, B.E., Perrichot, V., and Chaul, J.C.M. (2020). *Camelosphecia* gen. nov., lost ant-wasp intermediates from the mid-Cretaceous (Hymenoptera, Formicoidea). ZooKeys *1005*, 21–55.
13. Parker, J., and Kronauer, D.J.C. (2021). How ants shape biodiversity. Curr. Biol. *31*, R1208–R1214.
14. Latreille, P.A. (1802). Histoire naturelle des fourmis, et recueil de mémoires et d'observations sur les abeilles, les araignées, les faucheurs, et autres insectes (Crapelet).
15. Wilson, E.O., Carpenter, F.M., and Brown, W.L., Jr. (1967). The first Mesozoic ants. Science *157*, 1038–1040.
16. Engel, M.S., and Grimaldi, D.A. (2005). Primitive new ants in Cretaceous amber from Myanmar, New Jersey and Canada (Hymenoptera: Formicidae). Am. Mus. Novit. *3485*, 1–24.
17. Bolton, B. (2003). Synopsis and classification of Formicidae, *71* (Memoirs of the American Entomological Institute), pp. 1–370.
18. Economo, E.P., Narula, N., Friedman, N.R., Weiser, M.D., and Guénard, B. (2018). Macroecology and macroevolution of the latitudinal diversity gradient in ants. Nat. Commun. *9*. 1778-8.
19. Perrichot, V. (2019). New Cretaceous records and the diversification of the crown-group ants (Hymenoptera, Formicidae). In 8th International Congress on Fossil Insects, Arthropods, and Amber, Apr 2019 (Saint Domingue).
20. Wilson, E.O., Carpenter, F.M., and Brown, W.L., Jr. (1967). The first Mesozoic ants, with the description of a new subfamily. Psyche *74*, 1–19.
21. Futuyma, D.A. (2005). Evolution (Sinauer Associates, Inc. Publishers).
22. Perrichot, V. (2015). A new species of *Baikuris* (Hymenoptera: Formicidae: Sphecomyrminae) in mid-Cretaceous amber from France. Cretac. Res. *52*, 585–590.
23. Barden, P. (2017). Fossil ants (Hymenoptera: Formicidae): ancient diversity and the rise of modern lineages. Myrmecological News *21*, 1–30.
24. LaPolla, J.S., Dlussky, G.M., and Perrichot, V. (2013). Ants and the fossil record. Annu. Rev. Entomol. *58*, 609–630.
25. Théobald, N. (1937). Notes complémentaire sur les insectes fossiles oligocènes des gypses d'Aix-en-Provence. Bull. Mens. Soc. Sci. Nancy (n.s. *5*, 157–178.
26. Aria, C., Perrichot, V., and Nel, A. (2011). Fossil Ponerinae in Early Eocene amber in France. Zootaxa *2870*, 53–62.
27. Naora, N. (1933). Notes on some fossil insects from East-Asiatic continent, with descriptions of three new species, *1* (Entomology World Tokyo), pp. 208–219.
28. Wheeler, W.M. (1915). The ants of the Baltic Amber. Schr. Phys.-Ökon. Ges. Königsb. *55*, 1–142.
29. Dlussky, G.M. (1967). Ants of the genus *Formica* from the Baltic amber. Paleontol. Zh. *2*, 80–89.
30. Dlussky, G.M., and Rasnitsyn, A.P. (2009). Ants in the Upper Eocene amber of central and eastern Europe. Paleontol. J. *43*, 1024–1042.
31. Perkovsky, E.E. (2018). Only half of Rovno amber hymenopteran fauna is common with Baltic amber. Vestn. Zool. *52*, 353–360.
32. Larson, D.W., Brown, C.M., and Evans, D.C. (2016). Dental disparity and ecological stability in bird-like dinosaurs prior to the end-Cretaceous mass extinction. Curr. Biol. *26*, 1325–1333.
33. Barbosa, J.A., Kellner, A.W.A., and Viana, M.S.S. (2008). New dyrosaurid crocodylomorph and evidence for faunal turnover at the K–P transition in Brazil. Proc. Biol. Sci. *275*, 1385–1391.
34. Todd, J.A., Jackson, J.B.C., Johnson, K.G., Fortunato, H.M., Heitz, A., Alvarez, M., and Jung, P. (2002). The ecology of extinction: molluscan feeding and faunal turnover in the Caribbean Neogene. Proc. Biol. Sci. *269*, 571–577.
35. Smith, J.T., and Jackson, J.B.C. (2009). Ecology of extreme faunal turnover of tropical American scallops. Paleobiology *35*, 77–93.
36. Wilson, E.O., and Hölldobler, B. (2005). Eusociality: origin and consequences. Proc. Natl. Acad. Sci. USA *102*, 13367–13371.
37. Wilson, E.O., and Hölldobler, B. (2005). The rise of the ants: a phylogenetic and ecological explanation. Proc. Natl. Acad. Sci. USA *102*, 7411–7414.
38. Perrichot, V., Nel, A., Néraudeau, D., Lacau, S., and Guyot, T. (2008). New fossil ants in French Cretaceous amber (Hymenoptera: Formicidae). Naturwissenschaften *95*, 91–97.

39. Boudinot, B.E., Richter, A., Katzke, J., Chaul, J., Keller, R.A., Economo, E.P., Beutel, R.G., and Yamamoto, S. (2022). Evidence for the evolution of eusociality in stem ants and a systematic revision of †*Gerontoformica* (Hymenoptera: Formicidae). Zool. J. Linn. Soc. *195*, 1355–1389.

40. Arens, N.C., and West, I.D. (2008). Press-pulse: a general theory of mass extinction? Paleobiology *34*, 456–471.

41. Williamson, T.E., Brusatte, S.L., and Wilson, G.P. (2014). The origin and early evolution of metatherian mammals: the Cretaceous record. ZooKeys, 1–76.

42. Iba, Y., Mutterlose, J., Tanabe, K., Sano, S.I., Misaki, A., and Terabe, K. (2011). Belemnite extinction and the origin of modern cephalopods 35 my prior to the Cretaceous– Paleogene event. Geology *39*, 483–486.

43. Moon, B.C., and Stubbs, T.L. (2020). Early high rates and disparity in the evolution of ichthyosaurs. Commun. Biol. *3*. 68-8.

44. Perrichot, V., Wang, B., and Engel, M.S. (2016). Extreme morphogenesis and ecological specialization among Cretaceous basal ants. Curr. Biol. *26*, 1468–1472.

45. Zheng, D., Chang, S.C., Perrichot, V., Dutta, S., Rudra, A., Mu, L., Thomson, U., Li, S., Zhang, Q., Zhang, Q., et al. (2018). A Late Cretaceous amber biota from central Myanmar. Nat. Commun. *9*, 3170–3176.

46. Gallagher, A.J., Hammerschlag, N., Cooke, S.J., Costa, D.P., and Irschick, D.J. (2015). Evolutionary theory as a tool for predicting extinction risk. Trends Ecol. Evol. *30*, 61–65.

47. Magalhaes, I.L.F., Azevedo, G.H.F., Michalik, P., and Ramírez, M.J. (2020). The fossil record of spiders revisited: implications for calibrating trees and evidence for a major faunal turnover since the Mesozoic. Biol. Rev. *95*, 184–217.

48. Goloboff, P.A., and Catalano, S.A. (2016). TNT version 1.5, including a full implementation of phylogenetic morphometrics. Cladistics *32*, 221–238.

49. Ronquist, F., Teslenko, M., Van Der Mark, P., Ayres, D.L., Darling, A., Höhna, S., Larget, B., Liu, L., Suchard, M.A., and Huelsenbeck, J.P. (2012). MrBayes 3.2: efficient Bayesian phylogenetic inference and model choice across a large model space. Syst. Biol. *61*, 539–542.

50. R Core Team (2002). R: A language and environment for statistical computing (R Foundation for Statistical Computing). https://www.R-project.org/.

51. Oksanen, J., Blanchet, F.G., Kindt, R., Legendre, P., Minchin, P.R., O'hara, R.B., Simpson, G.L., Solymos, P., Stevens, M.H.H., Wagner, H., et al. (2013). Package 'vegan'. Community ecology package. version *2*, 1–295.

52. Roberts, D.W. (2007). labdsv: Ordination and multivariate analysis for ecology. R package version 1.

53. Carter, J.G., Gallagher, P.E., Valone, R.E., and Rossbach, T.J. (1988). Fossil collecting in North Carolina. Bulletin*89* (Department of Natural Resources and Community Development).

54. Lambert, J.B., Wu, Y., and Santiago-Blay, J.A. (2002). Modern and Ancient Resins from Africa and the Americas. In Archaeological Chemistry: Materials, Methods, and Meaning. ACS Symposium Series 831, K.A. Jakes, ed. (USA: American Chemical Society, Washington, District of Columbia), pp. 64–83.

55. Lambert, J.B., Tsai, C.Y.-h., Shah, M.C., Hurtley, A.E., and Santiago-Blay, J.A. (2012). Distinguishing amber classes by Proton Magnetic Resonance spectroscopy. Archaeometry *54*, 332–348.

56. Fedorov, A., Beichel, R., Kalpathy-Cramer, J., Finet, J., Fillion-Robin, J.C., Pujol, S., Bauer, C., Jennings, D., Fennessy, F., Sonka, M., et al. (2012). 3D Slicer as an image computing platform for the Quantitative Imaging Network. Magn. Reson. Imaging *30*, 1323–1341.

57. Abràmoff, M.D., Magalhães, P.J., and Ram, S.J. (2004). Image processing with ImageJ. Biophot. Int. *11*, 36–42.

58. Krynicki, V.E. (2013). Primitive ants (Hymenoptera: Sphecomyrminae) in the Campanian (Late Cretaceous) of North Carolina (USA). Life: The Excitement of Biology *1*, 156–165.

59. Nascimbene, P., and Silverstein, H. (2000). The preparation of fragile Cretaceous ambers for conservation and study of organismal inclusions. In Studies on Fossils in Amber, with Particular Reference to the Cretaceous of New Jersey, D.A. Grimaldi, ed. (Backuys Publishers), pp. 93–102.

60. Kolaceke, A., McKellar, R.C., and Barbi, M. (2018). A non-destructive technique for chemical mapping of insect inclusions in amber. PalZ *92*, 733–741.

61. Hölldobler, B., and Wilson, E.O. (1990). The ants (Harvard University Press).

62. Bolton, B. (1994). Identification guide to the ant genera of the world (Harvard University Press).

63. Lewis, P.O. (2001). A likelihood approach to estimating phylogeny from discrete morphological character data. Syst. Biol. *50*, 913–925.

64. Matzke, N.J., and Wright, A. (2016). Inferring node dates from tip dates in fossil Canidae: the importance of tree priors. Biol. Lett. *12*, 20160328.

Please cite this article in press as: Sosiak et al., Prolonged faunal turnover in earliest ants revealed by North American Cretaceous amber, Current Biology (2024), https://doi.org/10.1016/j.cub.2024.02.058

STAR★METHODS

KEY RESOURCES TABLE

REAGENT or RESOURCE	SOURCE	IDENTIFIER
Biological samples		
Fossil *Sphecomyrma nexa* holotype	American Museum of Natural History	AMNH-NC-515
Fossil *Brownimecia inconspicua* holotype	University of Kansas Natural History Museum	AMNH-NC-MSE-1
Fossil *Baikuris ocellantis* holotype	University of Kansas Natural History Museum	AMNH-NC-MSE-2
Deposited data		
Supplementary Information: additional figures and tables	Present study	supplemental information
Data S1: chronomorphospace morphometric data	Present study	Zenodo: https://doi.org/10.5281/zenodo.10637395
Data S2: generic persistence data	Present study	Zenodo: https://doi.org/10.5281/zenodo.10637395
Supplementary Dataset 3: phylogenetic matrices and outputs	Present study	Zenodo: https://doi.org/10.5281/zenodo.10637395
Supplementary Dataset 4: micro-CT scan and reconstruction data	Present study	Zenodo: https://doi.org/10.5281/zenodo.10637395
Software and algorithms		
TNT v.1.5	Goloboff and Catalano[48]	https://www.lillo.org.ar/phylogeny/tnt/
MrBayes v.3.2.7a	Ronquist et al.[49]	https://nbisweden.github.io/MrBayes/
R v.4.2.0	R Core Team[50]	https://cran.r-project.org/
R package *vegan*	Oksanen et al.[51]	https://github.com/vegandevs/vegan
R package *labdsv*	Roberts[52]	https://cran.r-project.org/web/packages/labdsv/index.html

RESOURCE AVAILABILITY

Lead contact

Further information and requests for resources and reagents should be directed to and will be fulfilled by the lead contact, Christine Sosiak (christine.sosiak@oist.jp).

Materials availability

The *Sphecomyrma nexa* specimen (AMNH-NC-515), *Baikuris ocellantis* (AMNH-NC-MSE-2), and *Brownimecia inconspicua* (AMNH-NC-MSE-1) are held by the American Museum of Natural History, New York City, New York, USA.

Data and code availability

Morphometric data, generic persistence data, phylogenetic data, and micro-CT scan and reconstruction data have been deposited at Zenodo and are publicly accessible as of the date of publication. DOIs are listed in the key resources table. All original code has been deposited at Zenodo and is publicly accessible as of the date of publication. The DOI is listed in the key resources table. Newly proposed names are registered under the following DOI numbers in Zoobank: *Sphecomyrma nexa* urn:lsid:zoobank.org:act:A99147BA-C13E-48A2-B413-8F1DAEF598EE; *Brownimecia inconspicua* urn:lsid:zoobank.org:act:DABB3380-CB35-4747-9CD1-573F61AAEAFB; *Baikuris ocellantis* LSIDurn:lsid:zoobank.org:act:A7F8A1CA-4FB1-48B3-9E0A-02B2E45FE223.

EXPERIMENTAL MODEL AND SUBJECT DETAILS

All described material was collected in North Carolina (USA) from an amber deposit in an Upper Cretaceous (Campanian) outcrop. The deposit is located along the Neuse River near Goldsboro, a locality that is part of the Cretaceous Black Creek Formation. The

Please cite this article in press as: Sosiak et al., Prolonged faunal turnover in earliest ants revealed by North American Cretaceous amber, Current Biology (2024), https://doi.org/10.1016/j.cub.2024.02.058

lower part of the unit is characterized by gray feldspathic sand with lenses of dark clay; the upper part consists of thinly interbedded dark clays with micaceous silty fine sand.[53] Amber from North Carolina has been designated as a Group A or B fossil resin based on nuclear magnetic resonance spectroscopy, suggesting that the botanical source is likely coniferous or a dipterocarp.[54,55]

METHOD DETAILS

Specimen preparation

Specimen AMNH-NC-515 was X-ray imaged at the American Museum of Natural History (AMNH) microscopy and imaging facility using a GE phoenix v|tome|x s240 CT-scanner. Scans were acquired using the machine's nano-focus 180 kV X-ray tube at 80kV and 250μA over 1 s exposure times and a voxel size of approximately 6.5μm. z stack files were generated with E phoenix datos|x software and volume reconstruction was undertaken using 3D Slicer v4.11[56] segmentation modules. Images of the reconstructed specimen were imported into ImageJ[57] for linear measurements of the traits, to retain consistency with measurements taken under stereo microscopy for other specimens.

The *Brownimecia* and *Baikuris* specimens were originally preserved in two centimeter-scale pieces of relatively clear, yellow amber that were hand-polished and epoxy-coated for stabilization using the technique described by Krynicki.[58] During the course of the study, it was necessary to embed the specimen AMNH-NC-MSE-1 in a larger block of epoxy and polish it closer to the inclusion to obtain taxonomically relevant views. The amber embedding technique used largely follows that outlined by Nascimbene and Silverstein.[59] AMNH-NC-MSE-1 was embedded in mineralogical-grade epoxy (Epotek-301) using a vacuum chamber; the sample was then cut and polished to remove excess material and provide a clearer view. Specimen AMNH-NC-MSE-2 was left in its original form and was observed under a glycerin bath to improve light transmission and correct distortions created by the curved outer surface of the amber. Preliminary analyses of the chemistry of the preserved cuticle in AMNH-NC-MSE-2 have been conducted as part of the work by Kolaceke et al.[60]

All observations for the *Brownimecia* and *Baikuris* specimens were made using a Leica MZ16 stereomicroscope and an Olympus CH30 compound microscope, both of which were equipped with options for transmitted, incident, and dark-field lighting. Photographs were prepared using a Visionary Digital macrophotography station, which consists of a Canon EOS 5D DSLR camera on a computer-driven stand with studio lighting. The Dun Ocellus lens was used (modified Canon EF 200 mm lens with Mitutoyo 5x, 10x, and 20x Plan Apo objective lenses). A vertical z stack series of images were taken of each specimen, and these were combined using Helicon Focus software in order to provide increased depth of field under high magnification. Specimen illustrations were completed using a graphic tablet, Sketchbook Pro, and Adobe Photoshop software, both tracing anatomical features directly from specimen photographs and making comparisons to the original specimens under a wide range of lighting conditions.

All measurements herein are given in millimeters and taken with an ocular micrometer. Anatomical terminology used follows that employed by Hölldobler and Wilson,[61] Bolton,[62] and Boudinot et al.[12] Institutional abbreviations: AMNH (American Museum of Natural History, New York City, New York, USA).

Specimen descriptions

Family Formicidae Latreille, 1802[14]

Subfamily Sphecomyrminae Wilson and Brown, 1967[15]

Genus *Sphecomyrma* Wilson and Brown 1967[15]

Type species

Sphecomyrma freyi Wilson and Brown 1967[15]

Included species

Sphecomyrma freyi Wilson and Brown 1967[15]; *S. mesaki* Engel and Grimaldi 2005[16]; *S. nexa* sp. nov.

Sphecomyrma nexa sp. nov.

Figures 1A, 1B, and S1.

Holotype

Specimen AMNH-NC-515 from Campanian amber of North Carolina. Single female worker, in small semi-cylindrical piece of dark yellow to orange amber, some fractures and resin textures obscuring specimen.

Diagnosis

Generally very morphologically similar to *S. freyi*, though distinct from *S. mesaki* in size and several morphological characters. *S. nexa* may be distinguished from *S. freyi* by the presence of an anterior-facing triangular spicule-like subpetiolar process in *S. nexa*, which *S. freyi* lacks; *S. freyi* additionally has a slightly more rounded petiolar node than *S. nexa*. The two species are extremely similar in size and proportion. *S. mesaki* is approximately twice the size of *S. nexa*; it may also be distinguished by a proportionally shorter scape in *S. mesaki*, and presence of an extended medial clypeal lobe in *S. mesaki*, which *S. nexa* lacks.

Description

Head. In frontal view, maximum head length from occiput to anterior margin of clypeus 1.07 mm; maximum width 0.96 mm excluding eyes. Cuticular texture smooth. Lateral and occipital margins broadly rounded in frontal view. Ocelli present, positioned in triangular pattern on vertex of head with lowest ocellus just above posterior-most margin of eyes in frontal view. Eyes large and oval, situated well above antennal sockets approximately halfway between sockets and posterior margin of head; maximum eye length 0.32 mm and width 0.24 mm. Eyes situated dorsad in lateral view, approximately $^{3}/_{4}$ total head depth. Genae broad, bowed

Please cite this article in press as: Sosiak et al., Prolonged faunal turnover in earliest ants revealed by North American Cretaceous amber, Current Biology (2024), https://doi.org/10.1016/j.cub.2024.02.058

in frontal view. Antennal sockets broadly inserted (distance between sockets 0.27 mm), abutting posterior margin of the clypeus; sockets situated within short and shallow cuticular depressions in head capsule ending just posterior to antennal sockets in frontal view. Frontal carina reduced. Torular sclerite flat, does not occlude the antennal socket. Clypeus large, width 0.68 mm and length 0.32 mm; lateral and medial epistomal sulci well defined; lateral epistomal sulci depart from medial epistomal sulcus at oblique angles. Lateral portions of clypeus quadrate, medial portion of anterior clypeal margin broadly convex, with small, pointed flange present at anterolateral clypeal margin above mandibular insertion. Mandibles curvilinear and simple, bidentate; basal tooth larger with sharp tip while apical tooth more blunted; deep groove present between denticles on external margin. Both maxillary and labial palps visible: maxillary palps 4-segmented with roughly equal lengths (proximal to distal: 0.15 mm, 0.14 mm, 0.19 mm, 0.16 mm); labial palps 3-segmented and roughly equal lengths (proximal to distal: 0.06 mm, 0.06 mm, 0.07 mm). Antenna 12-segmented, moderately long, 3-4x head length; scape short, does not reach posterior margin of head capsule. Funicles roughly equal in length with pedicel slightly shorter (0.18 mm), and flagellomere I (fal) which is longer than the rest (0.36). Antennal segment lengths as follows: scape 0.58 mm, pedicel 0.18 mm, fal 0.36 mm, faII 0.2 mm, faIII 0.2 mm, faIV 0.21 mm, faV 0.21 mm, fa VI 0.19 mm, faVII 0.19 mm, faVIII 0.19 mm, faIX 0.19 mm, faX 0.3 mm.

Mesosoma. Weber's length 1.48 mm. Dorsally, mesosoma bearing numerous fine upright setae and shorter appressed setae. Pronotum broad in dorsal view (width 0.62 mm); cuticular texture smooth. Propleuron approximately equal in depth to pronotum, broadly visible in lateral view and not occluded by pronotal sclerite; pleural texture punctate. Flexible promesonotal articulation present. Mesonotum elongate and shallow, descending steeply in lateral view, texture smooth. Metanotal sclerite present, ovoid in dorsal view (width 0.33 mm), flattened in lateral view from descent of mesonotum. Metanotal-propodeal suture heavily impressed. Meso-metapleural suture forming straight, diagonal line in lateral view. Propodeum broadly rounded with flattened dorsal surface in lateral view; gradually rounding into posterior propodeal margin, texture smooth. Metapleural gland visible posteroventrally, opening large and ovoid. At attachment of propodeum and petiole, propodeum terminates in slight upraised lip in lateral view. Procoxa elongate and rounded, length 0.62 mm, width 0.33 mm, cuticular texture punctate; meso- and metacoxa rounded and boxy, lengths respectively 0.37 mm and 0.49 mm, widths respectively 0.27 mm and 0.27 mm (measured ventrally), texture smooth. Trochantellus present. Femora elongate and flattened anteroposteriorly: profemur 1.12 mm long and 0.22 mm wide, mesofemur 1.0 mm long and 0.2 mm wide, metafemur 1.27 mm long and 0.21 mm wide. Tibia elongate and flattened anteroposteriorly: protibia 1.03 mm long and 0.14 mm wide, mesotibia 1.01 mm long and 0.13 mm wide, metatibia 1.19 mm long and 0.12 mm wide. Protibial spur large and simple; one simple and one pectinate mesotibial spurs; one simple and one pectinate metatibial spurs. Femora and tibia covered in fine, appressed setae. Five tarsal segments present on each leg; first tarsal segment much longer than other four which are roughly equal lengths. Mesotarsal lengths: tarsal segment I 0.59 mm, taII 0.23 mm, taIII 0.17 mm, taIV 0.11 mm, taV 0.15 mm. Pretarsal claws with medial subapical tooth.

Metasoma. Petiole broad and rounded dorsally, nodiform in shape, with node length 0.21 mm and height 0.51 mm. Subpetiolar process present just below anterior margin of node, process broad and quadrangular in lateral view and terminating in blunt spicule pointing anteriorly. Peduncle present but short. Posterior node surface shorter than anterior surface. Dorsal surface of petiolar node bearing numerous fine upright setae. Posteriorly, petiole narrows to attach ventrally to gastral segment I; helcium present. Gastral outline broadly tear-shaped. Cuticular texture smooth; tergites bearing numerous fine upright setae. Large, well-developed sting present.

Etymology

The specific epithet comes from the word "nexus" with the root Latin word *nectere* meaning "to bind", in reference to *Sphecomyrma's* status as the first described Mesozoic and stem ant species and its generalized morphology reflecting a "platonic ant" bauplan.

Remarks

S. nexa, while being morphologically similar to both known *Sphecomyrma* species, is exceptionally similar to *S. freyi*. However, the geographical and temporal separation of the two species, in combination with the presence of a subpetiolar spicule in *S. nexa*, allows differentiation between the two groups.

Genus *Baikuris* Dlussky, 1987[10]

Type species

Baikuris mandibularis Dlussky, 1987[10]

Included species

Baikuris casei Grimaldi, Agosti & Carpenter, 1997[8]; *B. mandibularis* Dlussky, 1987[10]; *B. maximus* Perrichot, 2015[22]; *B. mirabilis* Dlussky, 1987[10]; *B. ocellantis* sp. nov.

Baikuris ocellantis sp. nov.

Figures 1B, 1C and S2.

Holotype

Specimen AMNH-NC-MSE-2 from Campanian amber of North Carolina (Locality 34, lignite beds along the Neuse River in the region of Goldsboro, NC). Six apparently conspecific males within single piece of amber—holotype is centrally located within amber piece (i.e., "ant 1" of Krynicki[58]). Inclusions now in a flattened, reniform piece of amber that has been surface-polished and surface-coated with epoxy for stabilization, measuring approximately 14 mm.

Paratypes

Within same piece of amber as holotype (AMNH-NC-MSE-2), two additional largely complete specimens exist, one of which possesses clearer preservation of forewing venation than the holotype. Specimens AMNH-NC-MSE-2b and AMNH-NC-MSE-2c correspond to "ants 2 and 3" of Krynicki.[58]

Please cite this article in press as: Sosiak et al., Prolonged faunal turnover in earliest ants revealed by North American Cretaceous amber, Current Biology (2024), https://doi.org/10.1016/j.cub.2024.02.058

CellPress

Additional material

In addition to type material, specimen AMNH-NC-MSE-2 contains fragments of three additional individuals. The more complete specimens range from an isolated head to a relatively complete posterior section of the body, and correspond to "ants 4 and 5" of Krynicki.[58]

Diagnosis

In most regards, similar to *Baikuris casei*; however, new species differentiated by characters that include: rounded compound eyes that have flat anterior and posterior margins; markedly large ocelli; mandibles apparently toothless; palps long, with 6 maxillary palpomeres, and 4 labial palpomeres; single protibial spur simple and blade-like; two mesotibial spurs, one simple, and one denticulate; two metatibial spurs, with one simple and other blade-like; forewing with partially formed 2r-rs that is largely obscured by fuscous area in wing membrane apical to pterostigma; 1m-cu is interstitial, with its anterior juncture located at the split between Rs and M; gastral segment II larger than I; male genitalia strongly exposed, with setose parameres.

Description

In general, body of winged male with sparse setation, and apparent dark brown to black preservational colors where visible; total body length approximately 6.1 mm; head length ~0.8 mm; mesosomal length ~2.5 mm; gastral length ~2.1 mm.

Head. Impunctate and apparently glabrous; shape generally globose in outline, flattened posteriorly, without occipital carina; mouthparts project anteroventrally, and frontal area has medial convexity that matches curvature of clypeus. Compound eye round, with slightly flattened anterior and posterior margins; about 0.6 mm long. Ocelli very large and protuberant; lateral ocellus less than one ocellar diameter removed from margin of compound eye; interocellar spaces equivalent to slightly less than one ocellar diameter. Frontal area projecting anteriorly, forming low dome-shape, and toruli project anteriorly as well; toruli situated at middle of compound eye height. Scape and pedicel both relatively short; scape is cylindrical with slight posteriad curvature; pedicel pyriform, with swollen apex slightly wider than any subsequent flagellar articles; fal longest, longer than combined scape and pedicel; flagellomeres gradually and progressively diminish in length; holotype missing antennal apices, but paratype (AMNH-NC-MSE-2b) shows 11 antennal flagellomeres, with apical flagellomere ending in broadly rounded point. Palps long, with 6 maxillary palpomeres visible, and 4 labial palpomeres visible; labial palpomeres IV longer than combined II and III.

Mesosoma. This body region is poorly preserved in all available individuals; general proportions of mesosoma similar to those of *B. casei*. Pronotum relatively short, with triangular outline in lateral view; mesonotum protruding into posterior margin of pronotum extensively, with notauli deeply impressed; however posterior surface not clearly preserved and visible in samples available; scutoscutellar sulcus bearing faint foveae. Propodeum low-domed, with smooth dorsal surface resulting in little distinction between dorsal surface and posterior declivity; narrow shelf or carina forms collar around petiolar attachment, with shelf extending to form prominent square corner posterolaterally adjacent to metapleural gland opening; dorsal propodeal surface bearing dense coat of short, fine, recumbent setae; propodeal spiracle not clearly visible due to fragmentary cuticle preservation, but apparently slit-like. Legs with trochantellus present near base of all femora; protibial spur length 1.3 times apical width of protibia, blade-like and broad all the way to tip, with row of tiny stiff setae facing basitarsomere; mesotibial spurs both straight and short, with one spur slightly shorter than apical width of mesotibia, and other spur half of this length; metatibial spurs both slightly longer than apical width of metatibia. Tarsomeres on all feet with very short, decumbent spines dispersed across ventral surface—otherwise, legs have reduced pilosity, with exception of fine setae present on coxae; basitarsomere on hind leg longer than associated tibia; pretarsus on each foot bearing large arolium and pretarsal claws with single subapical tooth. Forewing venation overwhelmingly similar to that of *B. casei* (compare Figure 12B of Grimaldi et al., 1997[8] to Figures 1B, 1C and S2 herein). Primary differences in *B. ocellantis* include: C vein which appears to extend near base of pterostigma; prestigmal swelling of Sc+R vein appears substantial (although extent of stigma is difficult to discern due to partial preservation in all available specimens); abscissa 1Rs short, with length 0.4 times that of Rs+M; veins apical to abscissae Rs+M and 1CuA all appear somewhat nebulous instead of tubular; abscissa 2Rs gently curved, convex anteriorly; crossvein 2r-rs present as small stub extending from Rs, with length equal to width of adjacent Rs vein; junction between m-cu crossvein and M nearly in-line with 2Rs, almost eliminating 2M abscissa that is present in *B. casei*; 2CuA separated (from A) by bulla, and angled toward apex of wing, with distal extreme of vein curled adapically; fuscous area present within wing apex, extending from pterostigma to encompass 3M vein (dark area present within at least two preserved wings, but also potential taphonomic artifact).

Metasoma. Petiole largely cylindrical in dorsal view, with slightly convex dorsal surface; dorsal surface with dense coat of fine, subdecumbent and decumbent setae that are short but increase in length posteriorly. Posterior part of metasoma (gaster in classical terminology, metasomal segment II and posterior) drop-shaped with posterior part deflected anteroventrally; tergites with moderate coat of fine, short, decumbent setae. T1 bears longitudinal carina stemming from each anterolateral corner and extending slightly less than half of length. T2 longer than T1, with faint constriction between T1 and T2. Sternites bear coat of fine, moderately long, subdecumbent to erect setae, which become denser and more pronounced near posterior margins of posteriormost setae. Male genitalia exposed in 2 specimens and extended significantly, parameres clavate and short, with dense coat of erect setae reaching lengths greater than paramere width; penis valves with apical row of minute, erect setae; otherwise, genitalia difficult to observe.

Etymology

The specific epithet combines the Latin suffix *-antis*, or "giant" with ocellus, in reference to the large ocelli present within male members of the species.

Please cite this article in press as: Sosiak et al., Prolonged faunal turnover in earliest ants revealed by North American Cretaceous amber, Current Biology (2024), https://doi.org/10.1016/j.cub.2024.02.058

Remarks

The new species is very similar to *B. casei* from New Jersey amber, including sharing a large number of the diagnostic characters attributed to this species. However, the distinctive ocelli, partial crossvein 2r-rs, and toothless mandible allow *B. ocellantis* to be readily distinguished from the previously described taxon.

Subfamily Brownimeciinae Bolton, 2003[17]

Genus *Brownimecia* Grimaldi et al., 1997[8]

Type species

Brownimecia clavata Grimaldi et al., 1997[8]

Included species

Brownimecia clavata Grimaldi et al. 1997,[8] *B. inconspicua* sp. Nov.

Comments

All of the diagnostic characters originally proposed for *Brownimecia* are found within *B. inconspicua* n. sp., as well as the type species, *B. clavata*. An emended diagnosis for *B. clavata* that separates the two congeners includes: mandibles narrow apically and toothless, scimitar shaped; frontal area relatively flat, not strongly projecting anteriorly.

Brownimecia inconspicua sp. nov.

Figures 1D and S3.

Holotype

Specimen AMNH-NC-MSE-1 from Campanian amber of North Carolina (Locality 34, lignite beds along the Neuse River in the region of Goldsboro, NC). Single female worker with hemipteran syninclusions (probable Aphidoidea). Specimen now in a small, flat piece of yellowish amber, embedded in epoxy block measuring 8 mm.

Diagnosis

In general, with high degree of similarity to *B. clavata*. However, mandibles narrow and elongate, with broad, blunt apices extending near base of opposing mandible; frontal area bulbous and projecting anteriad; antenna with fal longer than pedicel; compound eye slightly larger (0.5 of head length); propodeum with posterior surface longer than dorsal surface; petiole longer and narrower than in *B. clavata* (in dorsal view); anterolateral corners of petiole bear fine longitudinal carinae on dorsal surface that extend one-third of petiolar length; metasomal segment III slightly longer than segment II, with cinctus on segment III.

Description

In general, body of worker (female) with sparse, short setae present on most dorsal surfaces and legs; total body length ~3.5 mm.

Head. Large, rounded, and inflated, except where it is recessed near dorsal margin of clypeus; compound eye small, slightly less than one-half of length of head (antero-posteriorly), and slightly protuberant; antennal insertions low on head, and widely separated from each other, positioned within trough formed dorsal to clypeus; ocelli not visible; occipital carina absent; head length ~ 0.8 mm. Antennae poorly preserved, with right antenna missing, and left antenna partially dismembered; scape elongate, reaching dorsal margin of compound eye, ~0.4 mm long; pedicel elongate and markedly narrow throughout basal half of its length, with total length ~0.1 mm; flagellomeres I to IV preserved attached to scape, all of which are pyriform in shape and gradually increasing in length; flagellomeres with dense coat of short, decumbent setae. Clypeus narrow (anteroposteriorly), and broad (laterally), with dorsal margin incised by antennal bases, and with row of chaetae along ventral margin. Mandibles elongate and narrow, with extensive overlap; left mandible overlapping right mandible near midlength when closed; broad mandibular apices lack any visible teeth, denticles, or chaetae, however chaetae may be hidden by cloudy amber emanating from oral cavity. Gena projects laterally near mandibular insertion, with small, rounded genal tooth. Labial and maxillary palps not visible due to large bubble emanating from mouth.

Mesosoma. General mesosomal outline is elongate and narrow; with pronounced neck created by elongate pronotum, and body strongly constricted by sharply incised metanotal groove; propodeum rounded, forming tall dome that extends dorsally to be even with mesonotum; total mesosomal length ~ 1.0 mm. Propodeum helmet-shaped as in *B. clavata*, but with pronounced lip surrounding posterolateral margin, forming narrow ledge; conical metathoracic spiracle present just posterior to metanotal groove; propodeal spiracle situated within posterior half of propodeum, and somewhat ventrally (i.e., closer to metapleural gland opening than in *B. clavata*); metapleural gland opening situated posterior to prominent transverse ridge (as in *B. clavata*: see Figure 9 of Grimaldi et al., 1997[8]), with dark guard hairs surrounding opening. Legs partially preserved; protibial spur gently curved, with blunt apex, extending slightly less than one-half of basitarsal length (Figure S3B); protibia also with longer, inclined setae present on ventral surface; metatibial spur long, blade-like, and relatively straight, slightly longer than apical width of metatibia; hind tibia also bears pair of short spines; probasitarsomere with subdecumbent, stiff setae that are as long as tarsomere is wide; pretarsal claws with robust subapical tooth positioned near midlength; large arolium present.

Metasoma. Petiole relatively long and narrow, with moderate dorsal convexity; dorsal surface of petiole gradually rises to posterior prominence, which is rounded and has slight medial impression that yields 'heart-shape' in dorsal view; single, elongate, suberect seta originates from each posterior 'lobe' of dorsal prominence. Gastral outline drop-shaped in lateral view, with shallow but well-defined constriction between gastral segments I and II; gastral length about 1.4 mm. Helcium not visible due to veil of bubbles in amber, but spacing of surrounding tergites supports its presence near mid-height of metasomal segment II; metasomal segment II narrower than in *B. clavata* (lateral margins are less convex); metasomal segment III longest, approximately 1.3 times length of segment II; relatively robust sting visible, slightly protruding from apex of metasoma (only visible using transmitted light), but details are largely obscured by cloudy amber and bubbles in this region.

Please cite this article in press as: Sosiak et al., Prolonged faunal turnover in earliest ants revealed by North American Cretaceous amber, Current Biology (2024), https://doi.org/10.1016/j.cub.2024.02.058

Etymology

The specific epithet comes from the Latin *inconspicuus*, or "hard to see", and refers to both the smaller compound eyes and mandibles without teeth found in this species.

Remarks

The new species and the known worker of *B. clavata*, are similar in size and morphology. Among the morphological differences, the easiest diagnostic characters to differentiate the new species from *B. clavata* are the presence of relatively spatulate mandibular apices, and the fact that the propodeum has a dorsal surface that is longer than the posterior surface, giving the appearance that the region extends dorsally on par with the dorsal surface of the promesonotum, and that metasomal III is the longest in *B. inconspicua*.

QUANTIFICATION AND STATISTICAL ANALYSES

Phylogenetic reconstruction

We assembled a morphological matrix spanning 65 worker characters and 48 taxa by incorporating two worker-based species described here into the matrix of Barden et al.[11] Taxonomic sampling comprised four non-ant aculeate outgroups, 24 crown-ants including the Cretaceous ant *Kyromyrma neffi*, and 20 stem ant terminals. The morphological matrix was optimized under equal weights parsimony using TNT v.1.5.[48] An initial agnostic search resulted in non-monophyly of congeners described here (species belonging to *Sphecomyrma* and *Brownimecia*) despite identical morphological coding for non-missing characters. We constrained monophyly of these taxa using the constraint and force commands, which resulted in trees of identical step sizes (scores of 214). We enforced monophyly of these congeneric terminals in two subsequent Bayesian Inference optimization searches, which we undertook in MrBayes v.3.2.7a[49]: one dated and one un-dated. While morphology-based divergence dating is not intended to provide an alternative to previous molecular-based estimates, we performed a tip-dating search to illustrate the temporal distribution of taxa studied here. As in Barden & Grimaldi[5] and Barden et al.,[11] we constrained the relationships of crown-ants based on recent molecular-based hypotheses of ant sub familial relationships.[3] We applied an Mkv + gamma model appropriate for morphology[63] by setting a gamma rate prior with variable coding. For the dated search, we specified a clock-constrained fossilized birth-death model as in Barden et al.,[11] which employed the flat prior values of Matzke &. Wright.[64] Fossil tip ages were set as fixed. Full MrBayes parameters are available in the supplemental data nexus files. Searches were run for five million generations under default chain and temperature settings. Convergence was assessed using reported split frequencies and estimated sample sizes >200 and 25% of sampled trees were discarded as burn-in.

Lineage longevity estimates

All lineage longevity estimates were made at the generic level. For fossil and extant taxa with an appropriate genus-level fossil record (i.e., occurrence in more than one fossil locality), minimum lineage longevity was estimated from the oldest appearance in the fossil record to the most recent appearance, or from the oldest appearance in the fossil record to 0 Ma for extant taxa. Including taxa reported here, three stem ant genera occur multiple times in the fossil record: *Sphecomyrma*, occurring from ~92 Ma to 75 Ma; *Brownimecia*, 92 Ma to 75 Ma; and *Baikuris*, 100 Ma to 75 Ma. We assessed crown lineage longevity in three separate categories: longevity for extinct crown lineages in the fossil record (crown genera with more than one fossil occurrence but no living members); extant crown lineage longevity in the fossil record; and extant crown lineage longevity from previously published phylogenetic estimates of generic divergence dates.

Morphometric analyses

To assess changes in morphology from stem lineages to crown lineages, we assembled a comprehensive dataset of stem and crown ant morphology. We sampled head width, head length, Weber's (mesosomal) length, and eye length from 443 worker specimens comprising 264 species. We included 21 species from stem ant lineages, spanning all known ages in the Cretaceous with associated fossil ant species, sampling from the Cenomanian, Turonian, and Campanian. Both *Sphecomyrma nexa* and *Brownimecia inconspicua* were included in morphospace construction; however, because *Baikuris ocellantis* is only represented by males, it could not be incorporated. The other 243 species were sampled from crown ant lineages, with 25 species sampled from the Eocene Baltic amber deposit, 50 species from the Miocene Dominican Republic amber deposit, and 167 species from extant lineages. Morphometric data were collected both directly from specimens by the authors and through surveys of the literature (Data S1). For most of the specimens, we were able to collate the full set of four measurements, but a few specimens from the literature were missing one measurement, predominantly from Eocene and Cretaceous deposits. If a specimen was missing more than one measurement, we excluded it from the dataset.

We performed principal coordinate analysis (PCoA) to evaluate changes in morphospace through time, as it illustrates maximum agnostic disparity within the dataset and can be implemented even with missing data. PCoA was implemented using generalized Euclidean distances to generate the disparity matrix. We subsampled the resultant morphospace by time slice; each fossil deposit was temporally age-independent from the others save the Charentese and Burmese amber deposits (100 Ma and 99 Ma respectively) which were clustered as one Cenomanian time slice. To better assess major morphological change through time, we constructed violin plots illustrating the change in median principal coordinate 1 and 2 scores through time. PCoA was implemented in R version 4.2.0,[50] using packages vegan[51] and labdsv.[52]